Regular Article

Rotational excitation of tetrahedral and octahedral molecules caused by electron and positron impact

Momentum transfer, integral and differential cross sections[*]

Marcos V. Barp[a] and Felipe Arretche

Departamento de Física, Universidade Federal de Santa Catarina, 88040-900 Florianópolis, Santa Catarina, Brazil

Abstract. Rotational excitation cross sections of tetrahedral and octahedral molecules caused by low energy positron/electron impact are the subject of this work. We developed a scattering model considering the Born approximation and the asymptotic multipole potential. These assumptions permitted us to achieve analytical expressions for rotational integral, momentum transfer and differential cross sections. We have found good agreement for positron and marginal agreement for electron interactions. The model can be improved with the inclusion of exchange effects and the distortion of the scattering wave function.

1 Introduction

The problem of electron and positron thermalisation in atomic and molecular gases finds motivation to be studied in many different branches of fundamental and applied science. For example, electron and positron collisions play a major role in the modelling of the energy deposition in planetary atmospheres [1], solar flares [2] and in the interstellar medium [3,4]. In the same fashion, annihilation radiation coming from the center of the galaxy [5] is a fascinating problem whose origin is still not fully understood. In the applied frontier, the modeling of swarm experiments [6] and plasmas always demanded the knowledge of electron cross sections with the chemical species present in the discharge environment [7]. More modernly, matter-antimatter plasmas received considerable attention [8] both in the applied and fundamental scenarios. Experimental initiatives toward the measurement of positron thermalisation times within molecular gases were performed by Al-Qaradawi et al. [9] and Natisin et al. [10] opening the possibility of generation of ultracold positron beams.

When high energy electrons and positrons get into molecular environments, they lose energy mainly by ionization [11] fastly cooling to energies of the order of ≈ 100 eV. Then, electronic excitation starts to compete

with ionization and the leptons cool until energies below the first inelastic electronic threshold, typically of the order of eV's for standard molecular gases [12]. After the electronic collision channels become energetically unavailable, vibrational excitation turns into the dominant energy loss mechanism. This situation persists until the particles reach energies of $\approx 10^{-1}$ eV, where vibrational excitation is no more allowed. For molecular gases at 300 K (≈ 0.025 eV), the leptons cool by elastic collisions but mainly by rotational excitation. Most of the cooling time is spent in this very low energy range, making the calculation and measurement of rotational excitation cross sections a fundamental step towards a deeper understanding of the thermalisation dynamics of electrons and positrons in molecular environments.

For an enlightening discussion about the scattering theory and its relevance in many branches of physics, we recommend the paper of Belkić [13]. Here we focus in the problem of rotational excitation caused by electron and positron impact. In particular, the paper of Itikawa and Mason [14] brings a good review for electrons. It is not hard to verify that the techniques to compute low-energy rotational excitation cross sections vary in two main aspects: the method to model the lepton-molecule interaction and the approach to incorporate the rotational dynamics in the scattering. Among many methods reported along the time in the literature of the field, and that were applied to compute rotational cross sections, we find the Schwinger Multichannel Method [15,16], the R-matrix [17], and the methods of Burke and Chandra [18] and Gianturco and Thompson [19]. Since these methods are highly dependent on computational processing, their

[a] e-mail: marcosbarp@gmail.com

application to bigger molecular systems demands constant analysis and computational processing strategies [20].

In particular, our group has devoted attention to this theme in the last years, calculating rotational excitation cross sections for positron-H_2, N_2, Li_2 [21–23] and tetrahedral molecules by positron impact [24] and rovibrational cross sections for electron-rare-gas dimers cross sections [25] using consecrated techniques like the adiabatic rotational approximation (ARA), the Born-multipole and zero range potential (ZRP) models, respectively. The attained experience in the works with H_2, N_2, Li_2 showed that simple analytical models, based on elementary assumptions, are useful to debug the codes, since they do not require high-end computational resources and allow one to vary the scattering and molecular parameters achieving results in real-time. In most occasions, the analytical models are capable to predict the qualitative value of a measure, and they permit us to observe if the high-level description methods are going in the right direction to perform a correct physical description of the scattering phenomenon.

This article is organized as follows: in Section 2 we briefly discuss the main aspects of the Born-multipole model; in Sections 3 and 4 we present our results, and finally, in Section 5 we state our conclusions. Atomic units are used unless otherwise explicit stated.

2 The Born-multipole model

In molecular physics, the geometry of the system strongly interferes in the way it interacts with the environment. Here we consider the rotational excitation of tetrahedral and octahedral molecules in the same way as discussed by Barp and Arretche [24]. In fact, this work is an extension of this last one, but focused in the discussion of results for momentum transfer and differential cross sections associated to rotational excitation. For the sake of completeness, we summarize the two main assumptions that compose the model:

1. the scattering amplitude is fairly calculated in the first Born approximation;
2. an effective one-body interaction potential can be taken from the multipole expansion of the many-body original potential.

From the considerations above, such methodology is usually denoted in literature as the Born-multipole model [26].

These hypothesis are easily justified in the context of positron-molecule scattering since the static potential is essentially repulsive. It means that the positron density decreases rapidly as the positron penetrates the molecular field. The electron-molecule static potential is, otherwise, attractive. But, due to the fact that the principal contribution to the rotational cross section comes from large distances of the incoming electrons from the molecule, the scattering wave function is only slightly distorted from its incident form and the Born approximation improves with decreasing incident electron energy [27]. In the Born approximation, if exchange interaction is disregarded, the

cross sections for electron and positron impact are the same. Moreover, the rotational cross sections are significantly smaller than the vibrational and elastic ones. In view of this fact, a perturbative approach providing analytical expressions is valuable.

The scattering amplitude for a rotational transition $\{J_i, K_i, M_i\} \rightarrow \{J_f, K_f, M_f\}$ (simply denoted from now on as "$i \rightarrow f$") becomes [24]

$$
\begin{aligned}
\mathcal{F}^{i \rightarrow f}[\boldsymbol{k}_f, \boldsymbol{k}_i] = &-\frac{1}{2\pi} \int d^3\boldsymbol{x}\, e^{-i(\boldsymbol{k}_f - \boldsymbol{k}_i)\cdot\boldsymbol{x}} \\
&\times \int d\Omega\, \Psi^{J_f}_{K_f M_f}{}^*(\Omega) \langle \chi_n(\boldsymbol{q})\,\Phi_0(\boldsymbol{r}_j; \boldsymbol{R}_A)|V \\
&\times |\Phi_0(\boldsymbol{r}_j; \boldsymbol{R}_A)\,\chi_n(\boldsymbol{q})\rangle \Psi^{J_i}_{K_i M_i}(\Omega),
\end{aligned} \qquad (1)
$$

where $\boldsymbol{x}$ denotes the projectile coordinates, $\boldsymbol{k}_f$ ($\boldsymbol{k}_i$) is the scattered (incident) projectile wave vector, the label J is related to the total angular momentum, K and M represent the projection of $\boldsymbol{J}$ in the z axis of the laboratory and body frames, respectively.

The effective potential, i.e.,

$$
\langle \chi_n \Phi_0 | V | \Phi_0 \chi_n \rangle = \sum_{l\,m} \frac{4\pi}{2l+1} q_{lm} \frac{Y_{l\,m}(\hat{x})}{x^{l+1}}, \qquad (2)
$$

is taken from the multipole expansion. Such potential is written in the body frame but the rotational transitions are recorded in the laboratory one, therefore we must transform $V(\boldsymbol{x})$ from the body to the laboratory referential. Besides that, since tetrahedral and octahedral molecules are spherical tops, the rotational wave functions are simply normalized Wigner matrices. Also, these systems present zero dipole and quadrupole moments. In fact the first non-zero moments are octupole, for tetrahedral, and hexadecapole, for octahedral molecules. For octupole and hexadecapole transitions, we have $l = 3$ and $l = 4$ in the multipole expansion of the scattering potential, as given in equation (2) above. The selection rules associated to these transitions are $J_f = J_i \pm 3$ and $J_f = J_i \pm 4$, respectively.

3 Tetrahedral systems

In this section, we shall consider only octupole transitions for CH_4 molecules. The reason to fix attention to this system lies in the fact that other authors reported results for rotational cross sections induced by electron and positron scattering for this molecule, with different methodologies and levels of coupling, making the comparison with our analytical results adequate for the purpose of this paper.

3.1 Positron scattering: rotational momentum transfer cross sections

In this section we report momentum transfer (diffusion) cross sections (σ_{MT}) associated to the rotational transitions for positron-CH_4. It differs appreciably from the rotational cross section (already reported in [24]) only
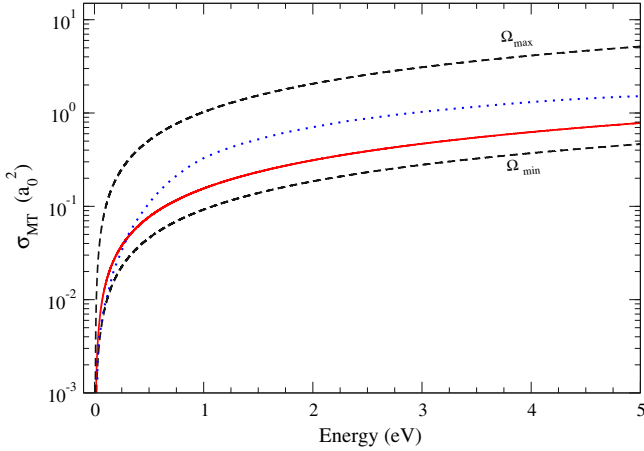
Fig. 1. Positron-CH$_4$ rotational momentum transfer cross section (σ_{MT}) for octupole transition ($0 \rightarrow 3$). We display our results with the lowest [30] ($\Omega_{\min} = 2.08$ ea$_0^3$) and highest [31] ($\Omega_{\max} = 8.3$ ea$_0^3$) octupole moments reported in literature, dashed lines. Also, we present our cross section with the octupole value of Isnard et al. [32] ($\Omega = 3.23$ ea$_0^3$), solid line. Our results are compared with the one of Jain and Thompson [29], dotted line.

when there is a pronounced scattering in either the backward or forward directions [28]. The expression for the momentum transfer cross section is given by

$$
\sigma_{\mathrm{MT}}^{J_i \rightarrow J_f} = \frac{k_f}{k_i} \frac{1}{(2J_i+1)^2} \sum_{M_i K_i} \sum_{M_f K_f} \frac{1}{4\pi}
$$
$$
\times \int d\hat{\theta} \int d\hat{\xi} \, (1 - \cos\theta) \, |\mathcal{F}^{i \rightarrow f}|^2
$$
$$
= \frac{1}{4\pi} \frac{k_f}{k_i} \frac{4}{(15)^2} \left(\frac{4\pi}{7}\right)^3 \left[k_i^2 + k_f^2 + \frac{2}{3} k_f k_i\right]
$$
$$
\times \left(\frac{2J_f+1}{2J_i+1}\right) \left[\frac{21}{5\pi} \langle\Omega\rangle^2\right], \tag{3}
$$

where θ is the angle between $\boldsymbol{k}_f$ and $\boldsymbol{k}_i$, and k_i and k_f are the absolute values of the initial and final wave vectors. Besides, an average of the initial state and a sum over the final states have been considered. Both solid angles $\hat{\theta}$ and $\hat{\xi}$ are discussed in reference [24]. Finally, $\mathcal{F}^{i \rightarrow f}$ is the scattering amplitude (see Eq. (1)) and Ω is the measured (or calculated) octupole moment. The notation $\langle\Omega\rangle$ means that an average over vibrational states is taken into account.

In Figure 1 we compare our results to the one of Jain and Thompson [29]. These authors considered a scattering potential constructed from the superposition of the static plus an ab initio nonparametric polarization potential.

The present calculation exhibits good agreement with the ab initio result of Jain and Thompson [29] at the low energy regime. This is expected based in the previous established conditions of the model. Furthermore, our result shows the same qualitative behaviour for energies far from the rotational threshold, when compared to the other theoretical calculation. This is also expected due

to the small contribution of partial waves with low l_i, i.e., $l_i = 0$. Indeed, it is possible to observe such contribution when a partial wave decomposition is performed (see Figs. 2 and 3 of Ref. [24]). In other words, the description of the potential inside the molecular region is important if the partial waves with $l_i = 0$ have significant contribution. Since $l_i = 0$ means frontal collision, the projectile gets deeper into the target potential field. Therefore, the discrepancy of the results in Figure 1 is strongly associated to the distortion of the scattering wave function.

3.2 Electron scattering: rotational integral and differential cross sections

In the electron scattering research field, it is well established that the exchange effect, not present in this model, plays an important role at low energies. Nevertheless, considering the scarce number of theoretical results, the lack of experimental data and, mainly, the considerable disagreement between the rotational integral and differential cross sections for tetrahedral molecules by electron impact, we consider that the report of the present results is valuable.

The rotational cross section can be calculated in the same way as the momentum transfer (1), disregarding the term $\cos\theta$ in equation (3).

Hence, the expression for the rotational integral cross section is [24]:

$$
\sigma^{J_i \rightarrow J_f} = \frac{1}{4\pi} \frac{k_f}{k_i} \frac{4}{(15)^2} \left(\frac{4\pi}{7}\right)^3 \left[k_i^2 + k_f^2\right] \left(\frac{2J_f+1}{2J_i+1}\right)
$$
$$
\times \left[\frac{21}{5\pi} \langle\Omega\rangle^2\right]. \tag{4}
$$

The expression for the rotational differential cross section (RDCS) for octupole rotational transitions is also readily obtained:

$$
\frac{d\sigma^{J_i \rightarrow J_f}}{d\theta} = \frac{k_f}{k_i} \left(\frac{2J_f+1}{2J_i+1}\right) \frac{32\pi \langle\Omega\rangle^2}{5^3 \, 7^4 \, 3} \left[k_i^2 + k_f^2 - 2k_f k_i \cos\theta\right]. \tag{5}
$$

The variables and labels present in equations (4) and (5) are the same as discussed in the previous section.

We compare our results to the theoretical values of Jain and Thompson [33], Brescansin et al. [34] and McNaughten et al. [35] for electron-CH$_4$. All these results were generated within the ARA. The rotational cross sections reported by Brescansin et al. [34] were calculated with the many body ab initio variational formulation known as Schwinger Multichannel Method. In such method the correlation-exchange effects between the incident electron and the target electrons are treated in the many body formalism, leading to a more complete and sophisticated description of the process. The results of Jain and Thompson [33] were derived by solving a set of coupled differential equations, taking into account an ab initio interaction potential where the exchange term is calculated with a free-electron-gas-exchange (FEGE) [36] model. Finally, McNaughten et al. [35] reported new results using the same formulation as
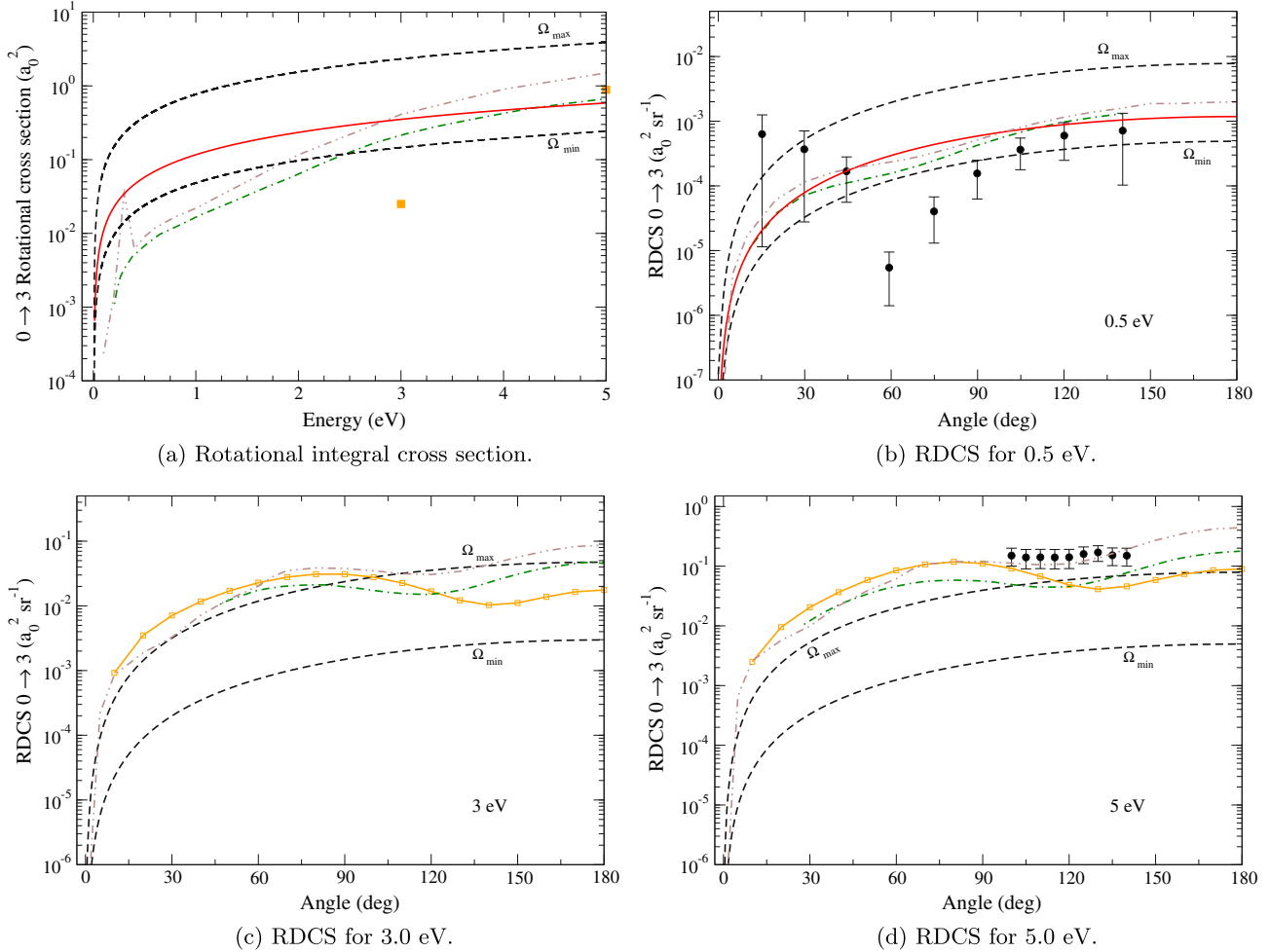
Fig. 2. Rotational integral and differential cross sections for octupole transition $(0 \rightarrow 3)$ in CH_4 for electron impact. Our results are shown for the lowest [30] ($\Omega_{min} = 2.08$ ea$_0^3$, dashed line with label) and the highest [31] ($\Omega_{max} = 8.3$ ea$_0^3$, dashed line with label) values for octupole moments reported in literature. We also used the value of Isnard et al. [32] ($\Omega = 3.23$ ea$_0^3$), solid line. Other theoretical results are: Brescansin et al. [34], squares (top left)/solid line with squares; Jain and Thompson [33], dashed-dotted; McNaughten et al. [35], dashed-dot-dot. The experimental values of Muller et al. [37] are represented by circles. (a) Rotational integral cross section. (b) RDCS for 0.5 eV. (c) RDCS for 3.0 eV. (d) RDCS for 5.0 eV.

Jain and Thompson [33] used, although applying an exact exchange model.

All results are summarized in Figure 2. It is noteworthy that the theoretical values for the integral rotational cross section, Figure 2a, show a considerable disagreement in the intermediary energies (see for example the data at 3 eV). The higher magnitude of our results when compared to the ones of Jain and Thompson [33] and McNaughten et al. [35] at low energies is probably due to the lack of exchange effects in the present model. At high energies, there is an agreement between the theoretical models, for example at 5 eV. At such energy, the distortion of the wave function and the description of the potential inside the molecular region are significant, thus the agreement of our calculation with the more elaborated models of interaction may be fortuitous, i.e. there may be a cancellation of factors that leads to such agreement.

For the differential cross section at 0.5 eV, Figure 2b, our results are in good agreement, when we compare

the magnitude, with the ones calculated by Jain and Thompson [33] and McNaughten et al. [35]. The slightly different behaviour in the differential cross sections is due to the description of the short-range interactions. All theoretical models are in disagreement with the only existing experimental data available in literature of Muller et al. [37] which exhibits a minimum at ≈ 60 degrees that is not observed in any theoretical calculation.

Comparing the results for 3 and 5 eV, respectively Figures 2c and 2d, they show a concordance in magnitude with the Born-multipole model if we consider the highest value of the octupole moment. The data from Brescansin et al. [34] exhibit a minimum structure between 120 and 140 degrees for both RDCSs which is observed but shifted to the region between 100 and 120 degrees in the other calculations. The experimental values of Muller et al. [37] are closer to the ones reported by McNaughten et al. [35]. It seems that the structure present at high angular region comes from the fact that for the forward scattering the
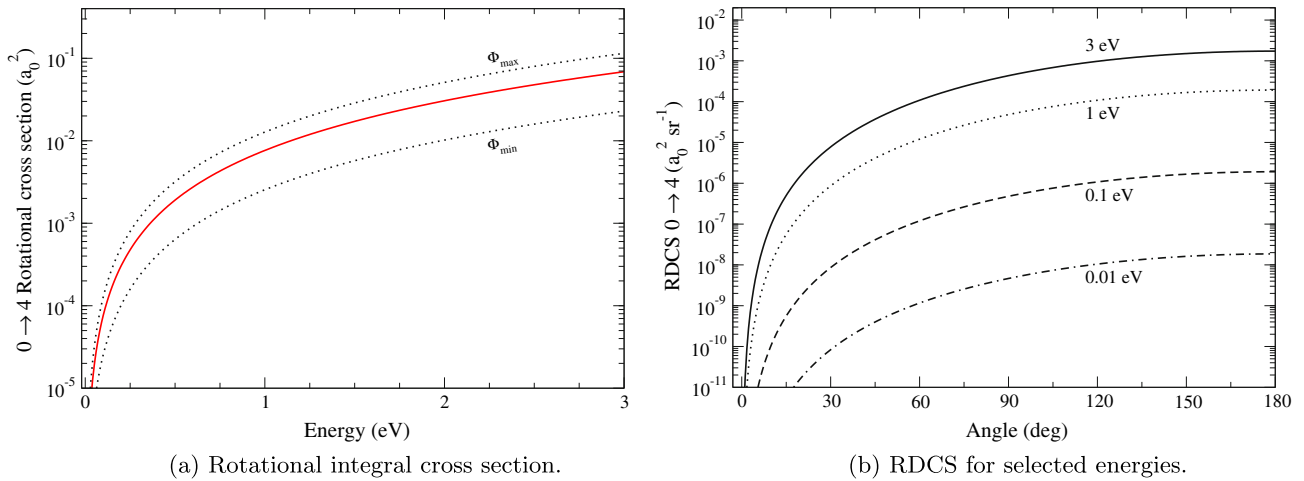
(a) Rotational integral cross section.

(b) RDCS for selected energies.

Fig. 3. Rotational integral and differential cross sections for hexadecapole transition $(0 \to 4)$ in SF_6 for positron/electron impact. Our results are shown for the lowest [40] ($\Phi_{min} = -14.3$ ea$_0^4$, dotted line with label) and the highest [41] ($\Phi_{max} = -32$ ea$_0^4$, dotted line with label) values for hexadecapole moments reported. The cross section obtained with the use of the value of Maroulis [42] ($\Phi = -24.76$ ea$_0^4$) is represented by a solid line in 3a and it was used for all curves of 3b. (a) Rotational integral cross section. (b) RDCS for selected energies.

short-range potential is important. Actually the different description of such effect by the other theoretical models displays the prominent influence of exchange for the backscattering effect.

4 Octahedral systems

The study of rotational transitions in octahedral molecules induced by positrons has a major role in the development of positron traps, since the SF_6 has been pointed out as the most efficient buffer gas [38,39]. However, neither experimental nor theoretical values are available for both rotational integral and differential cross sections.

The calculation can be performed similarly as done before (for more details see Sect. 3.2 of Ref. [24]). The rotational integral cross section is given by

$$\sigma^{J_i \to J_f} = \frac{1}{4\pi} \frac{k_f}{k_i} \frac{4}{(105)^2} \left(\frac{4\pi}{9}\right)^3 \left[\left(k_i^2 + k_f^2\right)^2 + \frac{4}{3}k_f^2 k_i^2\right]$$
$$\times \left(\frac{2J_f + 1}{2J_i + 1}\right) \left[\left(\frac{3}{2}\right)^2 \frac{1}{35\pi}\langle\Phi\rangle^2\right]. \quad (6)$$

Also, one can evaluate the rotational differential cross section by

$$\frac{d\sigma}{d\theta}^{J_i \to J_f} = \frac{k_f}{k_i} \left(\frac{2J_f + 1}{2J_i + 1}\right) \left(\frac{2}{35}\right)^3 \frac{\pi}{3^{10}}\langle\Phi\rangle^2$$
$$\times \left[k_i^2 + k_f^2 - 2k_f k_i \cos\theta\right]^2. \quad (7)$$

For both previous equations, $\langle\Phi\rangle$ is the hexadecapole moment and the other variables are the same as in equation (3).

Our calculation explicitly depends on the hexadecapole value. One may find in the literature a broad variation of

hexadecapole values for SF_6. Hence, we follow the same approach as aforesaid: we report the rotational integral cross section for the lowest and highest value in literature, i.e., -14.3 ea$_0^4$, from Birnbaum and Sutter [40], and -32 ea$_0^4$, from Isnard et al. [41]. In addition, after a careful review, we have used the value of -24.76 ea$_0^4$ from Maroulis [42] since in such work a complete investigation of the electric properties of SF_6 has been done.

We expect good agreement with further investigations in the positron area, since the rotational integral cross section is basically formed by high magnitude l_i partial waves (see Fig. 4 of Ref. [24]), which means that the inner part of the potential may be neglected. It is worth noting the importance of SF_6 in positron traps, since such molecule has been a subject of studies of positron accumulation and cooling for the creation of high-quality positron beams [38,43,44]. In the energy range of these experiments, the mechanisms responsible for energy loss by positrons are the momentum transfer, vibrational and rotational scattering. The relative relevance of each mechanism still being a matter of investigation.

In the electron sector, considering that the exchange effect is important, it is expected some discrepancy in the comparison of our results with more sophisticated models. Moreover, in the very low energy regime, since the dominant process involves nuclear motion [45–48], a fixed-nuclei approximation certainly will give qualitatively incorrect results for electron-SF_6 scattering.

According to reference [45], the lowest threshold for vibrational excitation of SF_6 is ≈ 0.1 eV. While electron attachment plays a very strong role for lower impact energies due to the nuclear motion of SF_6, there is no reason, at least in principle, to assume that positron attachment will have a similar relevance. In spite of the very low magnitude of the rotational excitation cross sections reported in Figures 3a and 3b, one may expect that the positron cooling in SF_6 gas will be dominated by momentum transfer

and rotational excitation, for energies below the vibrational threshold.

Finally, considering the limitations of the present scattering model, in the absence of resonances [49], the results reported in this paper shall give a fair estimate of the magnitude of the rotational excitation cross sections for SF_6.

5 Conclusions

We developed analytical expressions for the momentum transfer, integral and differential cross sections associated to octupole and hexadecapole rotational transitions. Such model depends only on the values of the octupole and hexadecapole moments, therefore it is possible to evaluate the rotational cross section for any tetrahedral and octahedral molecule, since these moments [42,50,51] are known and sophisticated computational approaches can be, at least in principle, readily debugged. Results for rotational excitation of CH_4 were systematically compared with previous calculations and experimental data. We have found good and marginal agreement for positrons and electrons, respectively. We have also reported results for SF_6, for further studies in buffer gases for positron traps [39,52].

In the case of electrons, it seems that the main reason for the discrepancy at low energy is the lack of the exchange effect, and, a proper description of the distortion of the scattering wave function.

Author contribution statement

All authors have contributed equally to the paper.

References

1. L. Gan, T. Cravens, Planet. Space Sci. **40**, 1535 (1992)
2. C.J. Crannell, G. Joyce, R. Ramaty, C. Werntz, Astrophys. J. **210**, 582 (1976)
3. J. Higdon, R. Lingenfelter, R. Rothschild, Astrophys. J. **698**, 350 (2009)
4. N. Guessoum, R. Ramaty, R.E. Lingenfelter, Astrophys. J. **378**, 170 (1991)
5. B. Johns, Modeling the galactic 511 kev positron annihilation emission, production, and propagation, All Dissertations, 652, 2010, https://tigerprints.clemson.edu/all_dissertations/652
6. R. Crompton, D. Gibson, A. McIntosh, Aust. J. Phys. **22**, 715 (1969)
7. Z.L. Petrović, S. Dujko, D. Marić, G. Malović, Ž. Nikitović, O. Šašić, J. Jovanović, V. Stojanović, M. Radmilović-Raenović, J. Phys. D: Appl. Phys. **42**, 194002 (2009)
8. A. Aksenov, R. Ruffini, G. Vereshchagin, Phys. Rev. Lett. **99**, 125003 (2007)
9. I. Al-Qaradawi, M. Charlton, I. Borozan, R. Whitehead, I. Borozan, J. Phys. B: At. Mol. Opt. Phys. **33**, 2725 (2000)
10. M.R. Natisin, J.R. Danielson, C.M. Surko, J. Phys. B: At. Mol. Opt. Phys. **47**, 225209 (2014)
11. S. Tao, J. Green, G. Celitans, Proc. Phys. Soc. **81**, 1091 (1963)
12. J. Marler, C. Surko, Phys. Rev. A **72**, 062713 (2005)
13. D. Belkić, J. Comput. Methods Sci. Eng. **1**, 353 (2001)
14. Y. Itikawa, N. Mason, Phys. Rep. **414**, 1 (2005)
15. K. Takatsuka, V. McKoy, Phys. Rev. A **24**, 2473 (1981)
16. J.S. Germano, M.A. Lima, Phys. Rev. A **47**, 3976 (1993)
17. J. Tennyson, Phys. Rep. **491**, 29 (2010)
18. P. G. Burke, N. Chandra, J. Phys. B: At. Mol. Phys. **5**, 1696 (1972)
19. F. Gianturco, D. Thompson, J. Phys. B: At. Mol. Opt. Phys. **13**, 613 (1980)
20. M. Gerdes, T. Barth, M. Grauer, J. Comput. Methods Sci. Eng. **3**, 463 (2003)
21. G.L. Zanin, W. Tenfen, F. Arretche, Eur. Phys. J. D **70**, 179 (2016)
22. M.V. Barp, E.P. Seidel, F. Arretche, W. Tenfen, J. Phys. B: At. Mol. Opt. Phys. **51**, 205201 (2018)
23. E.P. Seidel, M.V. Barp, W. Tenfen, F. Arretche, J. Electron. Spectrosc. Relat. Phenom. **227**, 9 (2018)
24. M. Barp, F. Arretche, J. Electron. Spectrosc. Relat. Phenom. **229**, 33 (2018)
25. E. Seidel, F. Arretche, Phys. Rev. A **98**, 052707 (2018)
26. K. Takayanagi, Y. Itikawa, The rotational excitation of molecules by slow electrons, in *Advances in Atomic and Molecular Physics* (Elsevier, 1970), Vol. 6, pp. 105–153
27. E. Gerjuoy, S. Stein, Phys. Rev. **97**, 1671 (1955)
28. H.S.W. Massey, E.H.S. Burhop, H.B. Gilbody, *Electronic and Ionic Impact Phenomena* (The Clarendon Press, Oxford, 1969), Vol. 1
29. A. Jain, D. Thompson, Phys. Rev. A **30**, 1098 (1984)
30. J.J. Sinai, J. Chem. Phys. **40**, 3596 (1964)
31. A.G. Turner, A.F. Saturno, P. Hauk, R.G. Parr, J. Chem. Phys. **40**, 1919 (1964)
32. P. Isnard, D. Robert, L. Galatry, Mol. Phys. **31**, 1789 (1976)
33. A. Jain, D. Thompson, J. Phys. B: At. Mol. Phys. **16**, 3077 (1983)
34. L.M. Brescansin, M.A.P. Lima, V. McKoy, Phys. Rev. A **40**, 5577 (1989)
35. P. McNaughten, D. Thompson, A. Jain, J. Phys. B: At. Mol. Opt. Phys. **23**, 2405S (1990)
36. S. Salvini, D. Thompson, J. Phys. B: At. Mol. Phys. **14**, 3797 (1981)
37. R. Muller, K. Jung, K.-H. Kochem, W. Sohn, H. Ehrhardt, J. Phys. B: At. Mol. Phys. **18**, 3971 (1985)
38. R.G. Greaves, C.M. Surko, Phys. Rev. Lett. **85**, 1883 (2000)
39. J. Danielson, D. Dubin, R. Greaves, C. Surko, Rev. Mod. Phys. **87**, 247 (2015)
40. G. Birnbaum, H. Sutter, Mol. Phys. **42**, 21 (1981)
41. P. Isnard, D. Robert, L. Galatry, Mol. Phys. **39**, 501 (1980)
42. G. Maroulis, Chem. Phys. Lett. **312**, 255 (1999)
43. R. Greaves, C. Surko, Nucl. Instrum. Methods Phys. Res. Sect. B **192**, 90 (2002)

44. D. Cassidy, S. Deng, R. Greaves, A. Mills Jr, Rev. Sci. Instrum. **77**, 073106 (2006)
45. L.G. Christophorou, J.K. Olthoff, J. Phys. Chem. Ref. Data **29**, 267 (2000)
46. C. Winstead, V. McKoy, J. Chem. Phys. **121**, 5828 (2004)
47. I.I. Fabrikant, H. Hotop, M. Allan, Phys. Rev. A **71**, 022712 (2005)
48. L. Gerchikov, G. Gribakin, Phys. Rev. A **77**, 042724 (2008)
49. M. Natisin, J. Danielson, G. Gribakin, A. Swann, C. Surko, Phys. Rev. Lett. **119**, 113402 (2017)
50. G. Maroulis, Chem. Phys. Lett. **259**, 654 (1996)
51. U. Hohm, G. Maroulis, J. Chem. Phys. **124**, 124312 (2006)
52. A. Banković, S. Dujko, S. Marjanović, R.D. White, Z.L. Petrović, Eur. Phys. J. D **68**, 127 (2014)